

HYPERLOOP MANCHESTER

**THE STUDENT-LED TRANSPORT
REVOLUTION**

**MAGNETIC LEVITATION
SUB- SYSTEM
Documentation**

HYPERLOOP MANCHESTER 2021/22

December 2021

Contents

1. System.....	3
1.1. Introduction	3
1.2. Principle Physics.....	3
1.3. Constraints.....	5
1.4. Complications with Other Subsystems	6
1.4.1. Issue with the changing height of the pod.....	6
1.4.2. Interference with electronics	6
1.4.3. Accommodating the braking system	6
1.5. Assembly.....	7
1.5.1. Magnets.....	8
1.5.2. Ski/Case	8
1.6. Active Maglev System	9
1.7. Testing of the System.....	9
1.7.1. Launcher Design.....	9
1.7.2. Passive System.....	10
1.7.3. Active System.....	10
2. References	11

1. System

1.1. Introduction

Most modern transport systems rely on wheels, which imposes a limit on the maximum velocities achievable due to friction. The solution involves lifting the pod up, to prevent direct contact with the track. Our system takes advantage of lenz's law, making use of permanent magnets moving over the conductive surface of the track. This moving magnetic field produces eddy currents in the track, which in turn creates its own magnetic field. which produces its own magnetic field. The interaction between the magnets and the induced magnetic field produces a force, directed upwards which is the lift that causes the pod to levitate.

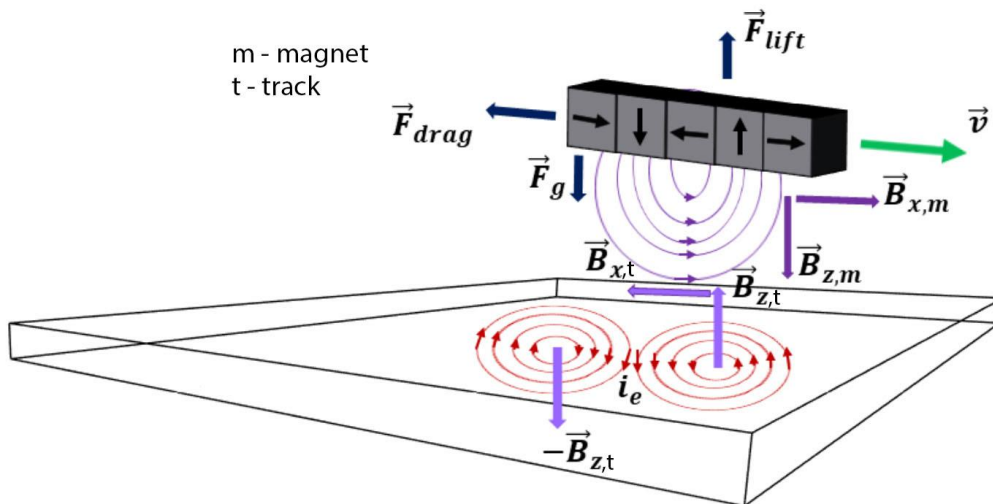


Figure 1. Overview of the forces involved in the system. (Adapted from: Chaidez, 2018, p.23)

1.2. Principle Physics

The strength of permanent magnets can be further increased by utilising a specific arrangement which is called a halbach array. It concentrates the magnetic field on one side, and almost negates it on the other (to a 0 in an ideal scenario). This is done by rotating the magnets as shown in figure 2. The number of magnets taken for one rotation of the halbach array is called the M number, which is =4 in the figure below.

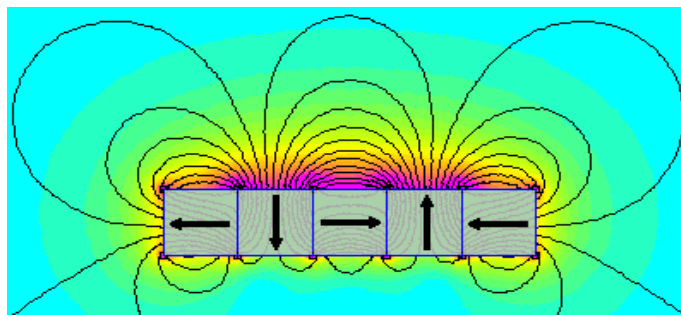


Figure 2. Halbach array arrangement (K&J Magnetics. Inc., 2021)

The peak magnetic field of the permanent magnet arrangement is represented by the equation below, where B_0 represents an exponential sine cardinal function (Post & Ryutov, 2000).

$$B_0 = B_r [1 - e^{-kd}] \frac{\sin\left(\frac{\pi}{M}\right)}{\left(\frac{\pi}{M}\right)} = B_r [1 - e^{-kd}] \text{sinc}\left(\frac{\pi}{M}\right)$$

Equation 1.

Here, d is the thickness of the permanent magnets, B_r , the natural permanent magnetic field of the permanent magnet material and k is the wave number which is related to the length of the array, λ as shown.

$$k = \frac{2\pi}{\lambda}$$

The lift force is the resultant from the cross-product of the induced magnetic field (+x-direction) and eddy currents in the y-direction. There is a slight drawback in this design however, as in any other. The magnetic force resultant from the cross-product of the induced magnetic field (+z-direction) and eddy currents in the y-direction causes drag which acts in the direction opposite that of the pod's velocity. This force hits a peak at a lower velocity and then converges to a minimum as the velocity increases.

The physical relationship is best represented as a Lorentz Force, where the cross product of a given magnetic field and moving charge will result in a force. As these formulations for the levitation and drag forces are sinusoidal in nature, an average of these force equations is taken. That is, an integration of $F_z(t)$ (vertical) and $F_x(t)$ (horizontal) can be taken over one periodic term of the excitation wave of the Halbach array, where $T = 2\pi\omega$. ω is the excitation frequency of the magnetic flux as a result of the speed of the moving magnetic field vectors ($\omega = kv$).

$$\langle F_z \rangle = \frac{1}{T} \int_0^T \vec{F}_z(t) dt = \frac{B_0^2 w_c^2}{2kL_c} \frac{1}{1 + \left(\frac{R_c}{\omega L_c}\right)^2} e^{-2k\Delta z}$$

$$\langle F_x \rangle = \frac{1}{T} \int_0^T \vec{F}_x(t) dt = \frac{B_0^2 w_c^2}{2kL_c} \frac{\left(\frac{R_c}{\omega L_c}\right)}{1 + \left(\frac{R_c}{\omega L_c}\right)^2} e^{-2k\Delta z}$$

Equation 2.1(top) and 2.2(bottom)

Here h_c , w_c , R_c , and L_c are track properties, namely the height, width, resistance and self-inductance. Δz is the levitation height

Another cause of inefficiency is the skin depth effect. Eddy currents are formed, primarily along the track surface, which in effect increases heat and resistance along the conducting track which contributes to loss in lift force, unless a special track is used, with discontinuous geometry. A single slab will ultimately suffer the effects of skin-depth.

Mathematically, skin-depth equates to the resistivity of the track, ρ , the angular frequency of the permanent magnet arrangement ω and the permeability constant of free space, μ -

$$\delta = \sqrt{\frac{2\rho}{\omega\mu_0}}$$

Equation 3.

Experiments conducted by the Lawrence Livermore National Laboratory have previously formulated a theoretical formula for accounting skin-depth of the lift formula. This modification is expressed as -

$$\langle F_{z,\delta} \rangle = F_{z,max} \frac{\left(\sqrt{1 + \frac{k^4\delta^4}{4} - \frac{k^2\delta^2}{2}}\right)^{3/2}}{k\delta + \left(\sqrt{1 + \frac{k^4\delta^4}{4} + \frac{k^2\delta^2}{2}}\right)^{3/2}}$$

Equation 4.

1.3. Constraints

- Based on the initial mass approximation of the pod, the system needed to be capable of providing a lift force of 250kgf or ~2450N
- We were allocated 1.6m of space along the length of the pod for our ski.
- The ski could not exceed the track width i.e. 127mm.
- Cruise speed provided by the propulsion system is 100 km/h or 27.78 m/s. Therefore, levitation was to be achieved at that speed.
- Allocated budget, including testing (**section 3.7**) - £2000

- The First set of special restrictions were imposed by the EHW rules, which prevent us from using certain 'zones' of the track
- Secondly, there are bump profiles on the flange and the web of the I beam track as per the rules.

Since the last document was submitted, the estimates changed. [

- the new pod weight estimate was 161.5 kgs
- the cruise speed was reduced to 60km/h due to track length and power limitations

1.4. Complications with Other Subsystems

1.4.1. Issue with the changing height of the pod

The initial suspension design had the wheels fixed in place, so the pod would go up/down by 10mm as the maglev system kicked in with changing velocity. The other subsystems faced difficulty accounting for this changing height, which led to us implementing retractable wheels in suspension.

The new system makes it, so the magnets are always at the same height above the track, and once the pod hits the cruise velocity, the wheels retract, allowing levitation to occur. There are still minor fluctuations in height due to slight variations in velocity during cruise, but they are within $\pm 1\text{mm}$.

1.4.2. Interference with electronics

The halbach array concentrates the magnetic field on one side and ideally reduces the component on the other to 0, but since an ideal version cannot be constructed, we must account for the small amount of flux on the opposing side. Even though the magnitude is very small, we must make sure that it does not interfere with any electronics/other systems who use magnets on board, especially the suspension system that is directly above the ski.

The solution requires us to introduce a back iron, which shortens the return path of magnetic flux as seen in the images in figure 4. It is generally used to increase the field strength on the opposing side, which is already being maximised with the halbach arrangement. So, our back iron only serves as a shield to prevent any interference.

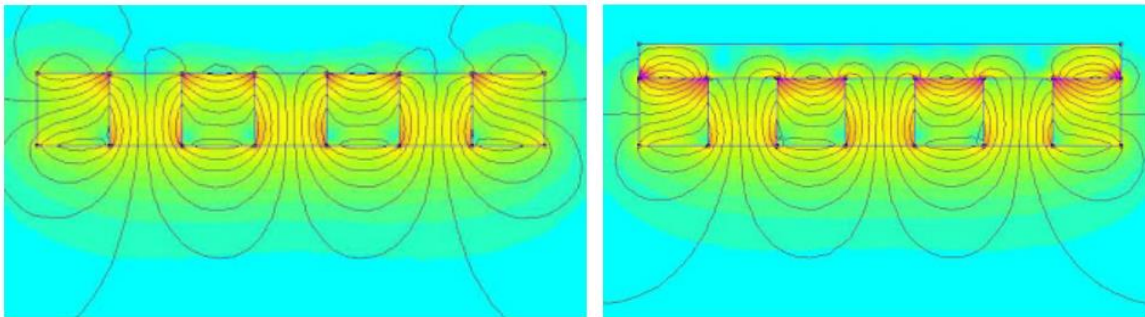


Figure 3. Halbach array (left) vs Halbach array with a back iron (right). (Parsons, R, 2018.)

1.4.3. Accommodating the braking system

The braking system uses friction brakes which clamp on both sides of the I-beam flange. The brakes also needed to be in the centre of the pod to avoid the pod from scraping the track. This means that the system needs space above the I beam, a minimum of 40mm clearance. The first maglev design iteration used 50mm magnets to achieve the required 40mm clearance, which allowed the braking system to sit beneath the ski.

A better solution that we came up with after submission of the ITS document makes use of a split ski design with the braking system in between. This greatly reduces the magnet size and number, which makes manufacturing much easier and leads to a decrease in costs.

1.5. Assembly

A MATLAB code was written using the formulas described in **section 1.2**. The lift force vs velocity was plotted for different magnet sizes and levitation heights. Number of magnets was maximised for each size based on the space availability. It was found that magnets sizes ($\geq 50\text{mm}$) would provide the necessary amount of lift force for the pod to levitate. Graphs for 20, 25 and 30mm magnets at 15mm levitation height, are given below.

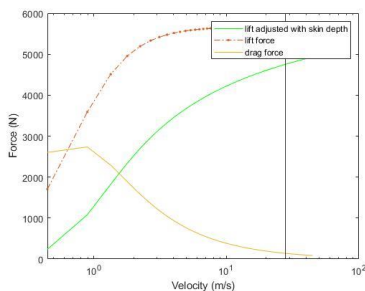


Figure 4. 30mm magnets plot

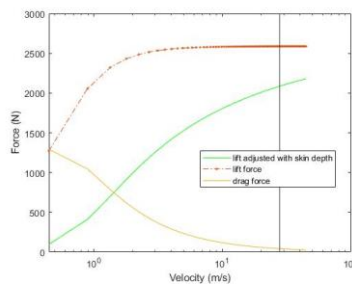


Figure 5. 20mm magnets plot.

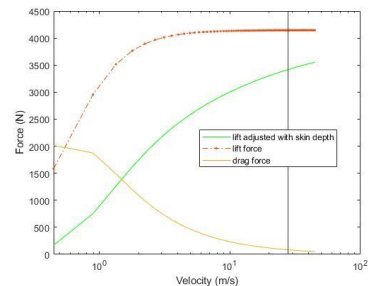


Figure 6. 25mm magnet plot

As you can tell, the shape of the plots are very similar. The only differences being

- The velocity at which peak drag force occurs
- Magnitude of the peak drag force
- The Lift force at cruise velocity, which is indicated using a vertical line on each graph.

Drag increases with increasing lift force so, we only had to find a setup that gave us an optimal lift force per our requirements.

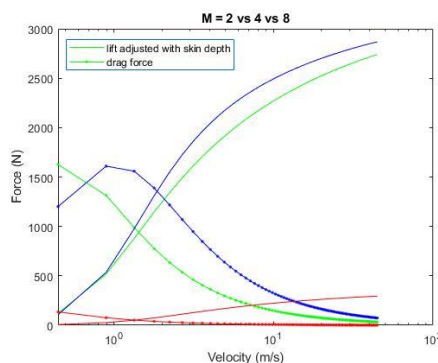


Figure 7. M number plot

$M = 8$ improved the performance by $\sim 10\%$ but, the added complexity during assembly (more like-poles grouped together compared to $M=4$) and the substantial increase in price made it impractical.

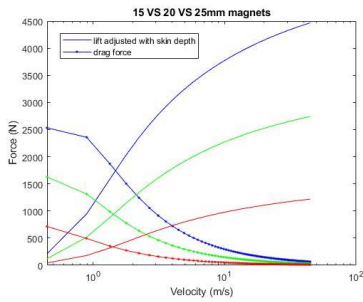


Figure 8. Magnet sizes plot

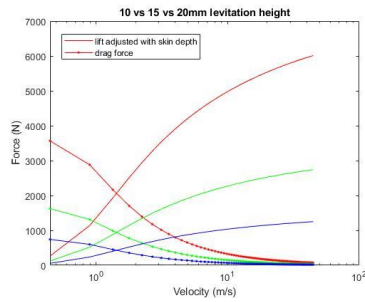


Figure 9. Levitation height plot.

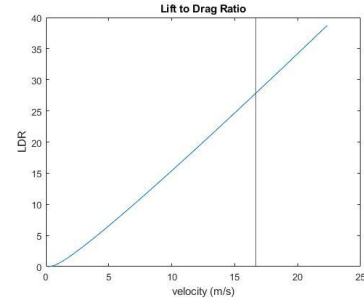


Figure 10. Lift to Drag ratio

Real world performance would not match our theoretical estimates despite accounting for the skin depth effect due to introduction of spacers to prevent magnet to magnet contact, possible defects in the assembly, increase in pod weight, propulsion team missing the target velocity. To account for this, we chose a setup which provides a lift force of $\approx 2460\text{N}$ at cruise speed as seen in **figure 11**. If the discrepancy isn't as big as we expect, and the propulsion system is up to spec, we can simply remove the necessary number of magnets to reach the required lift force.

1.5.1. Magnets

- 20mm cube, N52 neodymium magnets with a Ni-Cu-Ni coating.
- Δz (levitation height) = 15mm (base of magnet to top of the track)
- $M = 4$ i.e. each consecutive magnet is rotated by 90° .
- 24 magnets in total. 3x4 on either ski.

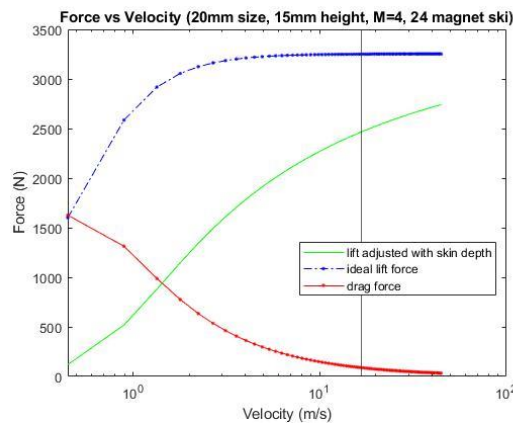
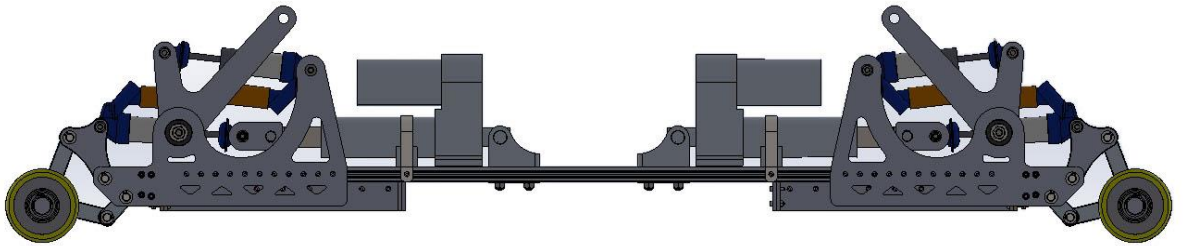


Figure 11. Final system specification

1.5.2. Ski/Case

- Casing made from a milled aluminium billet with 1cm thick walls.
- Back iron, 5cm thickness, on all sides except the bottom, to be bolted on to the case with m4 bolts.
- Since the ski is split in 2, there is an Extruded Aluminium Profile bridging the two.
- The case and back iron are mounted to the beam with m6 bolts.

- Finally, the magnets will be glued in with 1mm abs spacers to the casing using methyl methacrylate.



- *Figure 12. The MagLev ski incorporated in the current suspension design*

1.6. Active Maglev System

The system explained in this document is a form of a passive maglev system, which depends on linear velocity, v , for controlling its levitation gap. The active maglev system uses angular velocity to achieve the same functionality. This is done by translating the linear array to a circular one as shown in the figure below and spinning it at very high speeds.

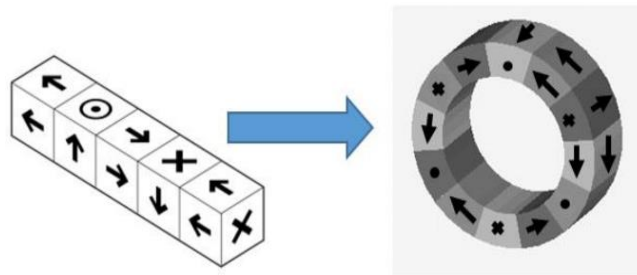


Figure 13. translation of linear to circular Halbach array (Chaidez, 2018, p.54)

The major advantage of this system is that levitation is not dependent on the pods velocity anymore, and a constant height can be maintained from rest up till the cruise velocity. Drag is still a factor, which now needs to be overcome by the motors responsible for spinning the array instead of the propulsion system of the pod. This system will be explored further, and likely replace the passive system in the next iteration of our pod.

1.7. Testing of the System

We plan on testing the system on a smaller scale before we commit to building it for the final pod.

To enable testing, a proprietary launching system had to be designed to launch the cart since we can't have a propulsion system on board, and off-the-shelf launchers are very expensive and would take too long to ship.

1.7.1. Launcher Design

The final specifications won't be determined before the submission of this document, but the principle will remain the same.

The system will use a pressurized chamber, which coupled with a quick exhaust valve (QEV) allows for a large amount of air to be released in a very short time, due to the QEVs short activation time, which provides a greater impulse and hence gives the cart a higher initial acceleration.

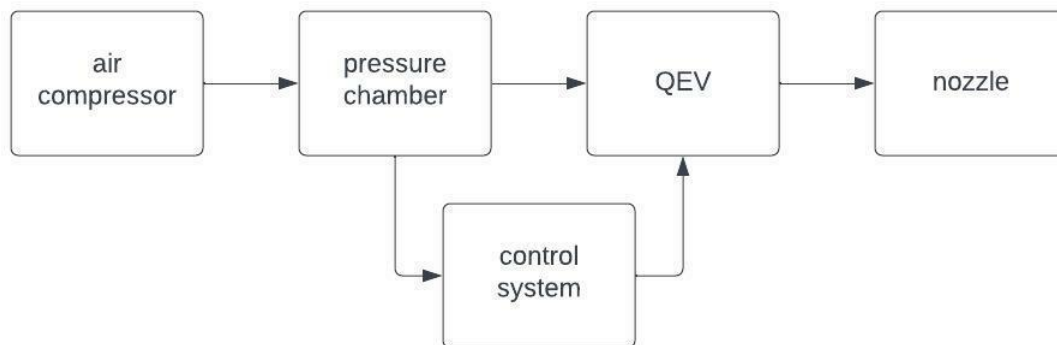


Figure 14. basic diagram showing connections of the launcher

1.7.2. Passive System

Three different setups of the system are going to be tested:

- Single ski of 10 mm magnets.
- Dual skis of 10mm magnets mounted side-by-side, to see if it is plausible to mount them in this configuration. Intuitively it should work, but we must test since no research has been published about dual Halbach arrays.
- single array of 25 mm magnets, to check how the force scales with magnet size

We will make use of height sensors and an accelerometer to measure and plot the height of the miniature vs speed. From this data, we will then be able to calculate the lift force from the magnets using **equation 2.1**. This will then be compared to the theoretical values, and the nature and amount of deviation can be calculated.

1.7.3. Active System

The active maglev system will also be tested to check feasibility. We will reuse the 10mm magnets and mount them in the circular configuration on a 3d printed case. Again, we will experiment with different arrangements, varying the radius and number of magnets. We can then use a high torque motor (to overcome the magnetic drag) to spin the assembly over an aluminium plate. The force can then be measured using a sensor placed under the plate and, readings can be taken for different angular velocities, and at different heights.

2. References

Apex Magnets. (2017) The Advantages and Disadvantages of Different Magnets[Online]. Available at: <https://www.apexmagnets.com/news-how-tos/advantages-disadvantages-different-magnets/>

[Accessed November 2021]

Chaidez, E. (2018) Modeling and Performance Evaluation of Electromagnetic Suspension Systems for the Hyperloop

Available at: <https://oaktrust.library.tamu.edu/handle/1969.1/173359>

[Accessed April 2021]

K&J Magnetics, Inc. Halbach Arrays [Online].

Available at: [Halbach Arrays \(kjmagnetics.com\)](https://www.kjmagnetics.com/halbach-arrays/)

[Accessed September 2020]

Parsons, R. (2018).The advantages and disadvantages of using a Halbach array with a BLDC (PMSM) motor

Available at: <https://things-in-motion.blogspot.com/2018/12/the-advantages-and-disadvantages-of.html>

[Accessed October 2021]

Post & Ryutov. (2000) The Inductrack Approach to Magnetic Levitation

Available at: <https://www.osti.gov/biblio/791522>

[Accessed 2020]